IL NUOVO CIMENTO **39 C** (2016) 400
DOI 10.1393/ncc/i2016-16400-1

Colloquia: IWM-EC 2016

Symmetry energy and composition of the outer crust of neutron stars

A. F. Fantina([1])([2]), N. Chamel([2]), J. M. Pearson([3]) and S. Goriely([2])

([1]) *Grand Accélérateur National d'Ions Lourds (GANIL), CEA/DRF, CNRS/IN2P3 Bvd Henri Becquerel, 14076 Caen, France*
([2]) *Institut d'Astronomie et d'Astrophysique, CP-226, Université Libre de Bruxelles (ULB) 1050 Brussels, Belgium*
([3]) *Dépt. de Physique, Université de Montréal - Montréal (Québec), H3C 3J7, Canada*

received 10 January 2017

Summary. — In this paper, we study the role of the symmetry energy on the composition of the outer crust of a neutron star. Although some correlations can be observed at the neutron-drip transition, the composition of the outer crust is mainly sensitive to the details of the nuclear structure far from the valley of stability rather than to the symmetry energy only.

1. – Introduction

Neutron stars (NSs) are among the most compact objects in the Universe, with central densities that can reach up to several times the nuclear matter density, $n_0 \approx 0.16\,\mathrm{fm}^{-3}$. They result from the gravitational core collapse of stars whose mass is greater than about 8–10 $M_\odot$ ($M_\odot$ being the mass of our Sun), at the end point of their evolution (see, *e.g.*, ref. [1]). Apart from a thin atmospheric plasma layer of light elements (mainly hydrogen and helium) possibly surrounding a Coulomb liquid of electrons and ions, the interior of a NS can be qualitatively divided into three regions: i) the outer crust, at densities above $\rho \approx 10^4$ g cm^{-3}, made of a crystal lattice of fully ionised atoms arranged in a body-centered cubic (bcc) lattice neutralised by a uniform degenerate electron gas (see, *e.g.*, ref. [2]); ii) the inner crust, above the neutron-drip density $\rho_{\mathrm{drip}} \approx 4 \times 10^{11}$ g cm^{-3} (see, *e.g.*, refs. [1-3]), composed of neutron-proton clusters immersed in a neutron liquid and neutralised by the degenerate electron gas; iii) a core, at densities above $\rho \approx 10^{14}$ g cm^{-3} (about half saturation density), composed by a homogenous liquid mixture of neutrons, protons, electrons, and, at higher densities, muons. In the innermost part, the composition is still a matter of debate, and additional particles like hyperons or deconfined quarks may exist (see, *e.g.*, ref. [1]).

The NS crust is also a unique nuclear physics "laboratory" to probe the properties of asymmetric nuclear matter, like the symmetry energy, at subsaturation density (see, *e.g.*, ref. [4]). The symmetry energy in infinite homogeneous nuclear matter is usually defined as

$$S_1(n) = \frac{1}{2}\frac{\partial^2(\mathcal{E}/n)}{\partial\eta^2}\bigg|_{\eta=0}, \tag{1}$$

where $\mathcal{E}(n,\eta)$ is the energy density of homogeneous nuclear matter with proton (neutron) density n_p (n_n), baryon density $n = n_n + n_p$, and charge asymmetry $\eta = (n_n - n_p)/n$. The symmetry energy can be also defined as the difference between the energy of pure neutron matter and that of symmetric matter. However, the two definitions do not exactly coincide, because of higher order terms in $\mathcal{E}(n,\eta)$ (see, *e.g.*, ref. [5]). Here, we will adopt the first definition, eq. (1), that can be expanded around n_0 as

$$S_1(n) \approx J + \frac{1}{3}L\left(\frac{n-n_0}{n_0}\right) + \frac{1}{18}K_{\rm sym}\left(\frac{n-n_0}{n_0}\right)^2 . \tag{2}$$

While the value of the symmetry energy at saturation, $J \approx 30\,\text{MeV}$, is rather well constrained by nuclear physics experiments, the value of its slope, L, or that of higher-order coefficients like $K_{\rm sym}$ are still poorly known (see, *e.g.*, refs. [6, 7]). Nevertheless, various studies have shown that the symmetry energy plays a role on the properties of the NS crust, like its composition, the crust-core transition, or the transition between the outer and inner crust (see, *e.g.*, ref. [8] and references therein).

In this paper, we study the role of the symmetry energy on the composition of the outer crust, for non-accreting and unmagnetised NSs, using a recent set of Brussels-Montreal microscopic nuclear mass models [9].

2. – Model of neutron-star crust

In the region of the crust considered here, the pressure is high enough that atoms are fully ionised [2]. Moreover, we assume that the temperature T is lower than the crystallisation temperature, so that nuclei are arranged in a regular bcc crystal lattice, that we consider made of only one type of ion ${}^A_ZX$, with mass number A and atomic number Z. The crystallisation temperature is usually much lower than the electron Fermi temperature. Therefore, electrons are highly degenerate, and can be treated as a uniform ideal relativistic Fermi gas. We also set $T = 0$. Expressions for the electron energy density and pressure, $\mathcal{E}_e$ and P_e, can be found in ref. [1]. The main corrections arise from electron-ion interactions (see, *e.g.*, ref. [10] for a discussion of other corrections; see also ref. [11] for a recent discussion on electron exchange and polarisation corrections to $\mathcal{E}_e$ and P_e that have not been included in the present work). Neglecting the finite size of ions and the quantum zero-point motion of ions off their equilibrium position, the lattice contribution to the energy density is given by $\mathcal{E}_L = Ce^2 n_e^{4/3} Z^{2/3}$, where C is a crystal structure constant ($C = -1.444231$ for a bcc lattice [12]), e is the elementary charge, and n_e is the electron number density (see, *e.g.*, ref. [1]). The total pressure reads $P = P_e + P_L$, where the lattice pressure is $P_L = \mathcal{E}_L/3$. The only microscopic inputs for the description of the outer crust are nuclear masses, which can be calculated from the corresponding atomic masses after subtracting out the binding energy of the atomic electrons (see eq. (A4) of ref. [13]). For the masses that have not yet been measured, we have used the microscopic mass tables computed by the Brussels-Montreal group (see, *e.g.*, ref. [14] for a recent review of these models).

The family of Brussels-Montreal nuclear mass models used here [9] are based on the nuclear energy density functional (EDF) theory using generalised Skyrme zero-range effective interactions [15], supplemented with a microscopic contact pairing interaction [16]. For these models, the masses of nuclei were obtained by adding to the Hartree-Fock-Bogoliubov (HFB) energy a phenomenological Wigner term and a correction term for the rotational and vibrational spurious collective energy [5]. The EDFs BSk22, BSk23, BSk24, BSk25, and BSk26 underlying the nuclear mass models HFB-22, HFB-23, HFB-24, HFB-25, and HFB-26, respectively, were fitted to the 2353 measured masses of nuclei with N, $Z \geq 8$ from the 2012 Atomic Mass Evaluation [17], with a root-mean-square (rms) deviation of about 0.5–0.6 MeV. Moreover, the incompressibility K_v of infinite homogeneous symmetric nuclear matter at saturation was required to fall in the range 240 ± 10 MeV [18], and the isoscalar effective mass was fixed to the realistic value $M_s^* = 0.8M$. These EDFs were also constrained to reproduce the equation of state (EoS) of homogeneous neutron matter, as obtained by many-body calculations using realistic interactions. Moreover, the EoSs of symmetric nuclear matter obtained from these EDFs are also compatible with the constraints inferred from the analysis of heavy-ion collision experiments [19, 20]. In constructing these five EDFs, BSk22 to BSk26, different values of the symmetry energy coefficient J were imposed thus making them suitable for a systematic study of the role of the symmetry energy on the properties of the NS crust. In particular, BSk22, BSk23, BSk24, and BSk25 have $J = 32$, 31, 30 and 29 MeV, respectively, and $L = 68.5$, 57.8, 46.4, and 36.9 MeV, respectively, and they were fitted to the realistic neutron-matter EoS labelled "V18" in ref. [21]. BSk26 was fitted to the EoS labelled "A18 + $\delta\, v$ + UIX*" in ref. [22] under the constraint $J = 30$ MeV, leading to a different value of $L = 37.5$ MeV at saturation with respect to BSk24. The values of J and L at saturation for all these EDFs are also consistent with those obtained from different theoretical and experimental constraints [6, 7]. Additional information on the value of J can be obtained from the recent measurement of ref. [23]. Indeed, Tarbert *et al.* inferred the diffuseness a_n and the half-height radius C_n of the neutron two-parameter Fermi distribution in ^{208}Pb, and thus the ^{208}Pb neutron-skin thickness $\Delta r_{np} = 0.15 \pm 0.03(\text{stat})$ fm, from coherent pion photoproduction cross section measurements. In fig. 1, we show this "experimental" constraint, together with the values of a_n and C_n predicted by the Brussels-Montreal EDFs BSk22 to BSk26 (dots). The outcome of these measurements tends to disfavour higher values of J. Incidentally, comparing various constraints from both nuclear physics and astrophysics [24, 25], BSk24 (BSk22) was found to be the best (worst) in the series of EDFs BSk22-BSk26. We will thus take BSk24 as "reference" model, while we will not consider the BSk26 EDF in the following analysis since it has been constrained to a different neutron-matter EoS. Furthermore, the values of the neutron-skin thickness in ^{208}Pb predicted by the EDFs BSk22 to BSk25 vary from 0.18 fm (BSk22) to 0.12 fm (BSk25), in agreement with the value extracted in ref. [23]. For all these reasons, we believe that these EDFs can be reliably applied to describe the NS crust.

3. – Numerical results

We have computed the properties of the outer crust of non-accreting unmagnetised NSs minimising the Gibbs free energy per nucleon at fixed pressure, as described in ref. [10]. We have increased the pressure with a step $\Delta P = 0.003\, P$. We have made use of the experimental masses from the 2012 Atomic Mass Evaluation [17] whenever available, complemented with the nuclear mass tables HFB-22 to HFB-25 from the BRUSLIB

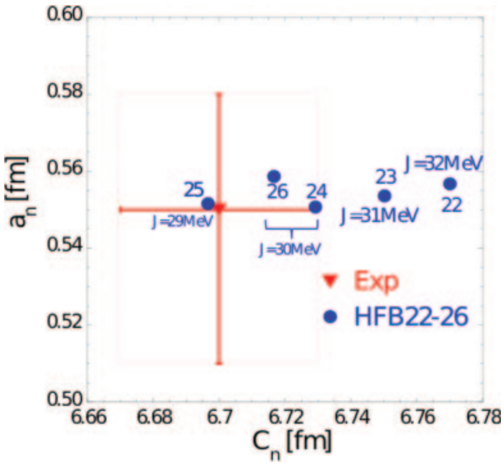

Fig. 1. – Diffuseness a_n *versus* half-height radius C_n for ^{208}Pb extracted from ref. [23]. Dots correspond to the values of a_n and C_n obtained with the Brussels-Montreal energy-density functionals BSk22 to BSk26 underlying the nuclear mass models HFB-22 to HFB-26.

database [26]. The composition of the outer crust predicted by the Brussels-Montreal models HFB-22 to HFB-25 is shown in table I. In bold are listed elements whose atomic mass is experimentally known [17]. Comparing the sequence of nuclei in table I, it can

Table I. – *Composition of the neutron-star outer crust as predicted by the Brussels-Montreal nuclear mass models HFB-22 to HFB-25* [9]. *In bold are elements whose atomic mass is experimentally known* [17].

HFB-22	HFB-23	HFB-24	HFB-25
^{56}**Fe**	^{56}**Fe**	^{56}**Fe**	^{56}**Fe**
^{62}**Ni**	^{62}**Ni**	^{62}**Ni**	^{62}**Ni**
^{58}**Fe**	^{58}**Fe**	^{58}**Fe**	^{58}**Fe**
^{64}**Ni**	^{64}**Ni**	^{64}**Ni**	^{64}**Ni**
^{66}**Ni**	^{66}**Ni**	^{66}**Ni**	^{66}**Ni**
^{86}**Kr**	^{86}**Kr**	^{86}**Kr**	^{86}**Kr**
^{84}**Se**	^{84}**Se**	^{84}**Se**	^{84}**Se**
^{82}**Ge**	^{82}**Ge**	^{82}**Ge**	^{82}**Ge**
^{80}**Zn**	^{80}**Zn**	^{80}**Zn**	^{80}**Zn**
^{79}Cu	–	–	–
^{78}Ni	^{78}Ni	^{78}Ni	^{78}Ni
^{80}Ni	^{80}Ni	^{80}Ni	–
^{124}Mo	^{124}Mo	^{124}Mo	^{124}Mo
^{122}Zr	^{122}Zr	^{122}Zr	^{122}Zr
^{121}Y	–	^{121}Y	^{121}Y
^{120}Sr	^{120}Sr	^{120}Sr	^{120}Sr
^{122}Sr	^{122}Sr	^{122}Sr	^{122}Sr
^{124}Sr	–	^{124}Sr	–
^{126}Sr	^{126}Sr	–	–
^{122}Kr	–	–	–

be noted that it is similar for the different models, apart from some missing nuclides. The discrepancies in the predicted nuclei arise from the uncertainties in the masses of neutron-rich nuclei. For example, HFB-22 predicts the existence of odd nucleus ^{79}Cu, contrarily to the other models. On the other hand, HFB-23 (HFB-25) does not support the presence of ^{121}Y (^{80}Ni), unlike the other models. The masses of ^{79}Cu calculated with HFB-22 and HFB-24 differ by only 700 keV, while for ^{80}Ni the difference in the theoretical mass calculated with HFB-25 and HFB-24 amounts to 750 keV. Finally, for ^{121}Y, the difference in the predicted mass between HFB-23 and HFB-24 amounts to 1.8 MeV. In ref. [9], it has been discussed how the masses of drip-line nuclei are correlated with J. Since mass is the only nuclear quantity on which the composition of the crust depends, it can be surprising that no correlation between J and composition is apparent. This correlation may be masked by the noise arising from the different errors with which the different EDFs fit the data and the numerical errors with which masses are calculated with a given EDF. Nevertheless, it is possible to establish some correlations between the properties of the crust at the neutron-drip transition and J (or L), as discussed in ref. [27]. Indeed, the Z/A ratio of the neutron-drip nucleus decreases with J, from 0.311 for HFB-25 to 0.295 for HFB-22. On the contrary, the neutron-drip density and pressure increase almost linearly with J, ranging from $n_{\rm drip} = 2.51 \times 10^{-4}\,{\rm fm}^{-3}$ for HFB-25 to $2.71 \times 10^{-4}\,{\rm fm}^{-3}$ for HFB-22 (the corresponding neutron-drip pressure varies from 4.83×10^{-4} MeV fm^{-3} for HFB-25 to 4.99×10^{-4} MeV fm^{-3} for HFB-22) (see ref. [27] for details).

4. – Conclusions

We have studied the role of the symmetry energy on the composition of the outer crust of a NS, using experimental atomic masses, complemented with accurately calibrated Brussels-Montreal nuclear mass models, from HFB-22 to HFB-25. The composition of the outer crust of a NS is very sensitive to the details of the nuclear structure far from the valley of stability. Around the neutron-drip transition, the composition is mainly determined by the masses of neutron-rich Sr and Kr isotopes. The small deviations in the compositions predicted by the different EDFs do not appear to be correlated with J. Nevertheless, correlations between the slope of the symmetry energy (or equivalently J) and the properties of the NS crust at the neutron drip can be observed.

* * *

This work has been supported by Fonds de la Recherche Scientifique - FNRS (Belgium), NSERC (Canada), and the COST Action MP1304 "NewCompStar".

REFERENCES

[1] Haensel P., Potekhin A. Y. and Yakovlev D. G., *Neutron Stars 1: Equation of State and Structure* (Springer, Berlin) 2007.
[2] Chamel N. and Haensel P., *Living Rev. Relativ.*, **11** (2008) 10.
[3] Chamel N., Fantina A. F., Zdunik J. L. and Haensel P., *Phys. Rev. C*, **91** (2015) 055803.
[4] Steiner A. W., Prakash M., Lattimer J. and Ellis P. J., *Phys. Rep.*, **411** (2005) 325.
[5] Goriely S., Chamel N. and Pearson J. M., *Phys. Rev. C*, **82** (2010) 035804.
[6] Tsang M. B., Stone J. R., Camera F. *et al.*, *Phys. Rev. C*, **86** (2012) 015803.

[7] Lattimer J. M. and Lim Y., *Astrophys. J.*, **771** (2013) 51.
[8] Baldo M. and Burgio G. F., *Prog. Part. Nucl. Phys.*, **91** (2016) 203.
[9] Goriely S., Chamel N. and Pearson J. M., *Phys. Rev. C*, **88** (2013) 024308.
[10] Pearson J. M., Goriely S. and Chamel N., *Phys. Rev. C*, **83** (2011) 065810.
[11] Chamel N. and Fantina A. F., *Phys. Rev. D*, **93** (2016) 063001.
[12] Baiko D. A., Potekhin A. Y. and Yakovlev D. G., *Phys. Rev. E*, **64** (2001) 057402.
[13] Lunney D., Pearson J. M. and Thibault C., *Rev. Mod. Phys.*, **75** (2003) 1021.
[14] Chamel N., Pearson J. M., Fantina A. F. *et al.*, *Acta Phys. Pol. B*, **46** (2015) 349.
[15] Chamel N., Goriely S. and Pearson J. M., *Phys. Rev. C*, **80** (2009) 065804.
[16] Chamel N., *Phys. Rev. C*, **82** (2010) 061307(R).
[17] Audi G., Wang M., Wapstra A. H. *et al.*, *Chin. Phys. C*, **36** (2012) 1287.
[18] Colò G., Giai N. V., Meyer J. *et al.*, *Phys. Rev. C*, **70** (2004) 024307.
[19] Danielewicz P., Lacey R. and Lynch W. G., *Science*, **298** (2002) 1592.
[20] Lynch W. G. *et al.*, *Prog. Part. Nucl. Phys.*, **62** (2009) 427.
[21] Li Z. H. and Schulze H.-J., *Phys. Rev. C*, **78** (2008) 028801.
[22] Akmal A., Pandharipande V. R. and Ravenhall D. G., *Phys. Rev. C*, **58** (1998) 1804.
[23] Tarbert C. M., Watts D. P., Glazier D. I. *et al.*, *Phys. Rev. Lett.*, **112** (2014) 242502.
[24] Pearson J. M., Chamel N., Fantina A. F. and Goriely S., *Eur. Phys. J. A*, **50** (2014) 43.
[25] Fantina A. F., Chamel N., Pearson J. M. and Goriely S., *AIP Conf. Proc.*, **1645** (2015) 92.
[26] `http://www.astro.ulb.ac.be/bruslib`.
[27] Fantina A. F., Chamel N., Mutafchieva Y. D. *et al.*, *Phys. Rev. C*, **93** (2016) 015801.